

BISTABILITY IN A HYPERCHAOTIC SYSTEM WITH A LINE EQUILIBRIUM

Chunbiao Li^{a}, J. C. Sprott^{b**}, Wesley Thio^{c***}*

^a*School of Information Science and Engineering, Southeast University
210096, Nanjing, China*

^b*Department of Physics, University of Wisconsin-Madison
53706, Madison, WI, USA*

^c*Department of Electrical and Computer Engineering, The Ohio State University
43210, Columbus, OH, USA*

Received October 26, 2013

A hyperchaotic system with an infinite line of equilibrium points is described. A criterion is proposed for quantifying the hyperchaos, and the position in the three-dimensional parameter space where the hyperchaos is largest is determined. In the vicinity of this point, different dynamics are observed including periodicity, quasi-periodicity, chaos, and hyperchaos. Under some conditions, the system has a unique bistable behavior, characterized by a symmetric pair of coexisting limit cycles that undergo period doubling, forming a symmetric pair of strange attractors that merge into a single symmetric chaotic attractor that then becomes hyperchaotic. The system was implemented as an electronic circuit whose behavior confirms the numerical predictions.

DOI: 10.7868/S0044451014030197

1. INTRODUCTION

Equilibrium points are some of the most fundamental properties of dynamical systems, and they play an important role in the bifurcations that occur. Frequently, systems have more than one equilibrium point [1–5], and if these equilibria are stable, they have basins of attraction whose boundaries can be very complicated. Under certain conditions, there can be a continuum of equilibrium points, for example, spread along a finite or even infinite line with different points on the line having different stability properties [6, 7]. Such line equilibria can occur in chaotic systems where the line is surrounded by a strange attractor and influences its dynamics. However, the case where a line equilibrium

occurs in a hyperchaotic system in largely unexplored. Furthermore, the phenomenon of multistability is an important feature in nature and is found to occur, for example, in low levels of quanta [8] and in the Taylor–Green dynamo [9].

Hyperchaos was first described by Rössler [10] in a four-dimensional system with two unstable equilibrium points. Other hyperchaotic systems have no equilibria [11, 12], one equilibrium [13], or five equilibrium points [14]. It is thus natural to ask whether there are hyperchaotic systems with infinitely many equilibrium points. In [15], hyperchaos was recently found in a four-dimensional memristive system with a line of equilibria, which contains one cubic and three quadratic nonlinearities. In this paper, we provide a new example of such a system that exhibits hyperchaos over a large region of parameter space in the presence of an infinite line of equilibrium points. Significantly, this system has only quadratic nonlinearities and a relatively large region of bistability, where a coexisting symmetric pair of limit cycles turns into strange attractors that then merge into one symmetric strange attractor before it becomes hyperchaotic or a symmetric pair of strange attractors merge or remerge between two hyperchaotic regions.

*E-mail: chunbiaolee@gmail.com; Also at Engineering Technology Research and Development Center of Jiangsu Circulation Modernization Sensor Network, Jiangsu Institute of Commerce, Nanjing 210007, China; Department of Physics, University of Wisconsin-Madison, Madison, WI 53706, USA

**E-mail: sprott@physics.wisc.edu

***E-mail: wesley.thio@gmail.com

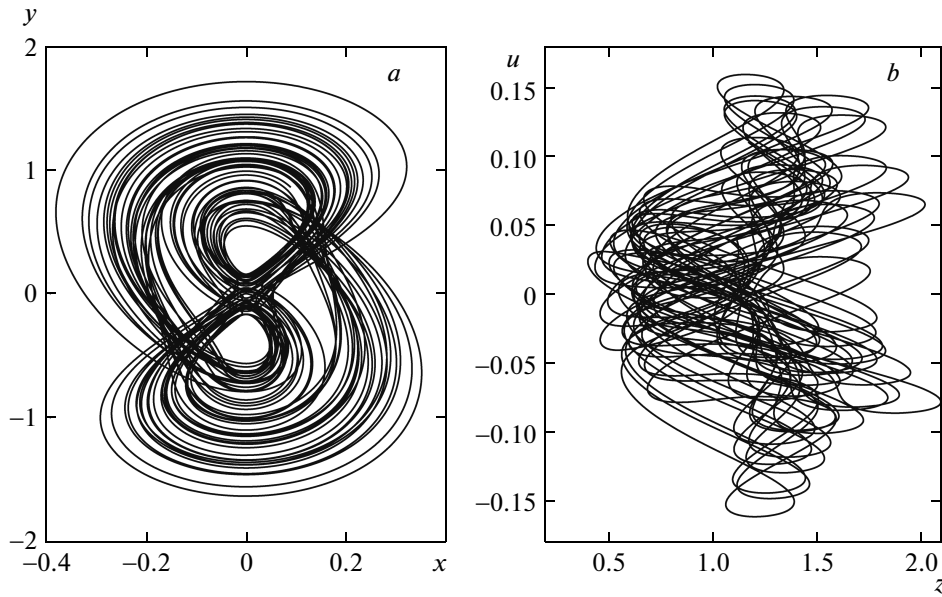


Fig. 1. Hyperchaotic attractor observed from system (2) with $a = 5$, $b = 0.28$, and $c = 0.05$ for the initial conditions $(0, 0, 0.8, 0.02)$ (a) xy plane, (b) zu plane

2. HYPERCHAOTIC FLOW WITH A LINE EQUILIBRIUM

2.1. Dynamical analysis and basic properties

Systems with several quadratic terms are most likely to have an infinite line of equilibrium points. A similar three-dimensional flow with six terms and a single linearity as reported in [7],

$$\begin{aligned} \dot{x} &= y - xz - yz, \\ \dot{y} &= axz, \\ \dot{z} &= y^2 - bz^2, \end{aligned} \tag{1}$$

which has chaos for some parameters, such as $a = 4$ and $b = 0.3$. System (1) has two equilibrium points at $(0, \pm\sqrt{b}, 1)$ and an infinite line of equilibrium points at $(x, 0, 0)$. Correspondingly, by introducing an additional dimension with linear feedback in the above system, a four-dimensional system with a line of equilibria is obtained,

$$\begin{aligned} \dot{x} &= y - xz - yz + u, \\ \dot{y} &= axz, \\ \dot{z} &= y^2 - bz^2, \\ \dot{u} &= -cy. \end{aligned} \tag{2}$$

The corresponding Jacobian matrix is

$$J = \begin{pmatrix} -z & 1 - z & -x - y & 1 \\ az & 0 & ax & 0 \\ 0 & 2y & -2bz & 0 \\ 0 & -c & 0 & 0 \end{pmatrix}. \tag{3}$$

When $a, b, c, z \neq 0$, system (2) has the full rank because the determinant of the Jacobian matrix is $2abcz^2$, which means that system (2) is a truly four-dimensional system. If any of a, b, c, z are zero, then the system reduces to one whose dimension is less than four.

The rate of hypervolume contraction is given by the Lie derivative,

$$\nabla V = \frac{\partial \dot{x}}{\partial x} + \frac{\partial \dot{y}}{\partial y} + \frac{\partial \dot{z}}{\partial z} + \frac{\partial \dot{u}}{\partial u} = -(2b + 1)z. \tag{4}$$

Hence, system (2) is dissipative with solutions that contract as time goes to infinity onto an attractor of zero measure in the four-dimensional state space whenever the time average of z is positive and $b > -0.5$.

The system has only the real line equilibrium $(x, 0, 0, 0)$ if the parameters a, b, c are not zero, and the corresponding eigenvalues are $(0, 0, 0, 0)$, which shows that the equilibrium is nonhyperbolic and the system lies on a bifurcation point and is nonlinearly unstable. For the initial conditions $(y_0, z_0) = (0, 0)$, the dynamics become one-dimensional, given by $\dot{x} = u_0$, and therefore the orbit is unbounded for $u_0 \neq 0$.

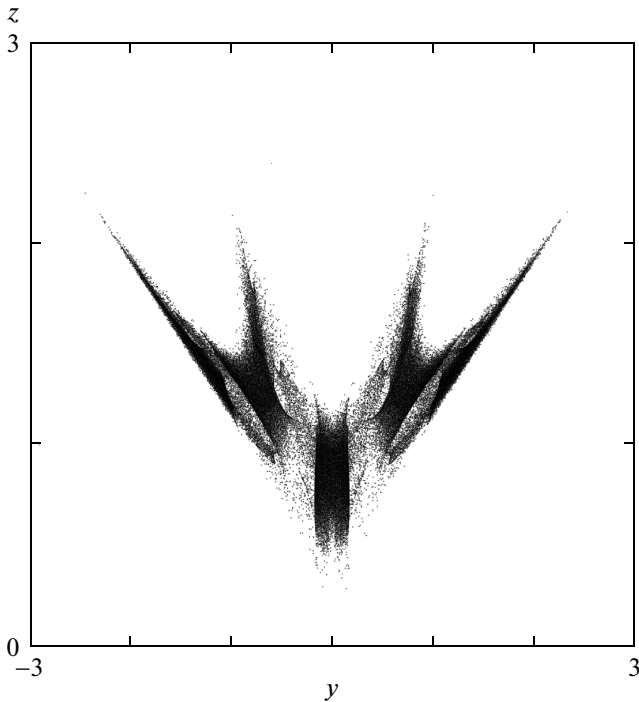


Fig. 2. Projection onto the yz plane of a cross section of the attractor at $x = 0$ for system (2) with $a = 5$, $b = 0.28$, and $c = 0.05$ and initial conditions $(0, 0, 0.7, 0.01)$

Like the three-dimensional system (1), system (2) has rotational symmetry with respect to the z axis, as evidenced by its invariance under the coordinate transformation

$$(x, y, z, u) \rightarrow (-x, -y, z, -u),$$

which means this four-dimensional system could also have symmetric pairs of coexisting attractors, such as limit cycles or strange attractors.

2.2. Hyperchaotic attractor

The degree of hyperchaos can be quantified by the value of the second largest Lyapunov exponent normalized to the most negative exponent. By this criterion, the maximum hyperchaos is found to occur for $a = 5$, $b = 0.28$, and $c = 0.05$, where the Lyapunov exponents are $(0.0750, 0.0366, 0, -1.6617)$ and the Kaplan–Yorke dimension is $D_{KY} = 3.0672$. The hyperchaotic attractor in different projections is shown in Fig. 1. System (2) is clearly four-dimensional because it has four distinct Lyapunov exponents and a cross section in the hyperchaotic region whose dimension is at least 2.0, as shown in Fig. 2.

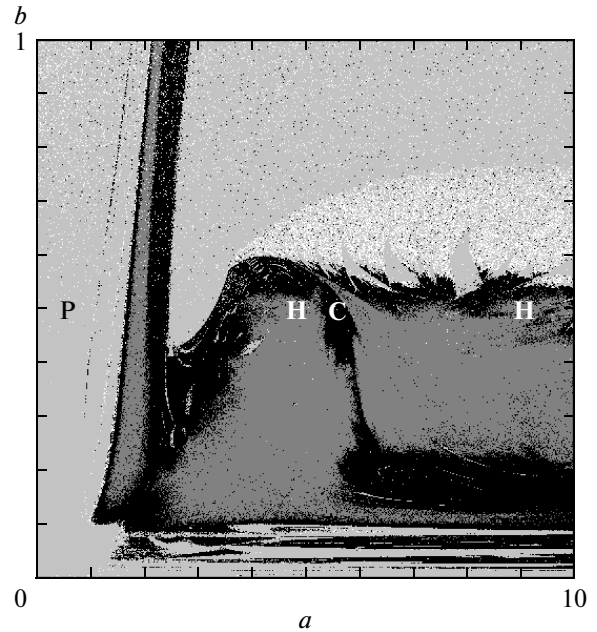


Fig. 3. Regions of various dynamical behaviors as a function of the bifurcation parameters a and b . The hyperchaotic regions are in dark grey, the chaotic regions are in black, the quasiperiodic regions are in light-light grey, and the periodic regions are in light grey

2.3. Dynamical regions

System (2) has eight terms and thus three parameters. For $c = 0.05$, regions of different dynamical behaviors in the a, b parameter space are shown in Fig. 3. In this calculation, each pixel uses a different random initial condition chosen from a Gaussian distribution of mean zero and variance 1.0. Thus the dotted regions, which suggest the coexistence of attractors of different types, are actually long transients. In particular, the dense region of light-light dots corresponds to a torus (quasiperiodic) attractor. There are large regions where the system is hyperchaotic with those regions surrounded by chaos (black), such that there is no way for the system to transition directly to hyperchaos from periodicity or quasiperiodicity.

A counter-intuitive feature is that the Kaplan–Yorke dimension is relatively small when the hyperchaos is large, whereas the maximum Kaplan–Yorke dimension occurs for $a \sim 300$, $b \sim 0.07$, and $c = 0$, where the system becomes three-dimensional with an extraneous equation and a constant u given by the initial condition u_0 , for which the greatest Kaplan–Yorke dimension occurs at $u_0 = 0$. For these conditions, the Lyapunov

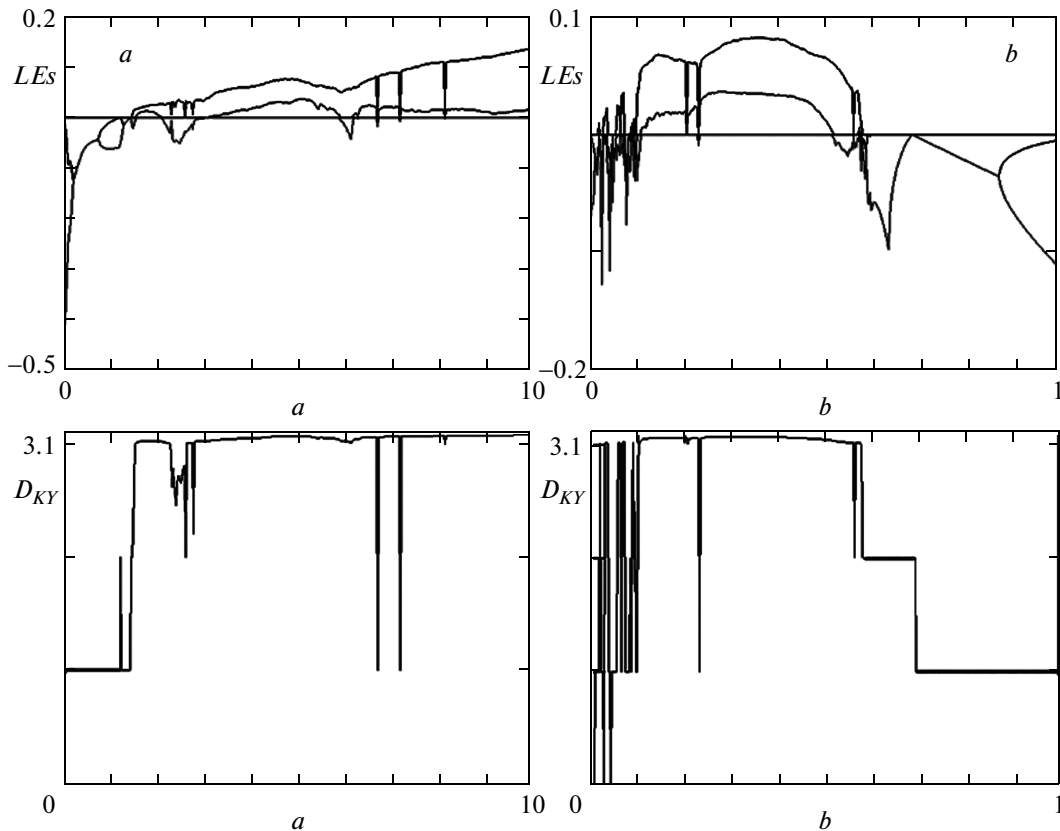


Fig. 4. Largest three Lyapunov exponents of system (2) with $c = 0.05$ and their respective Kaplan–Yorke dimensions. (a) $b = 0.28$, versus a , (b) $a = 5$, versus b

Lyapunov exponents are $(0.05632, 0, -1.7901)$, and the corresponding Kaplan–Yorke dimension is $D_{KY} = 2.3146$ in the three-dimensional space or $D_{KY} = 3.3146$ in the four-dimensional space, where the extraneous dimension gives an additional zero Lyapunov exponent.

3. BISTABILITY AND ATTRACTOR MERGING

Generally, chaotic flows with involutorial symmetries have either a single symmetric attractor or a symmetric pair of coexisting attractors. To explore the bifurcations of system (2), we take slices through Fig. 3 for fixed b and fixed a . The corresponding Lyapunov exponents and their respective Kaplan–Yorke dimensions are shown in Fig. 4.

When $b = 0.28$ and $c = 0.05$, as a increases, a symmetric limit cycle splits at $a \approx 1.08$ into a symmetric pair of limit cycles that evolve into a symmetric

pair of strange attractors that merge into a single symmetric strange attractor, which then unmerges before remerging and becoming hyperchaotic with a similar Kaplan–Yorke dimension, as shown in Fig. 5.

When $a = 5$ and $c = 0.05$, as b decreases from 1.0, system (2) becomes hyperchaotic through the limit cycle, torus, and chaos, which are shown in Fig. 4 as distinct steps in the Kaplan–Yorke dimension.

In Fig. 3, there is a nearly vertical band of chaos (black) with an embedded region of hyperchaos (dark grey), which can be approximately described by the function

$$b = 2.5a - 5.25.$$

This band apparently stretches to infinity and separates the periodic regions (light grey) into two different areas. The left area consists of a symmetric limit cycle that becomes hyperchaotic after a narrow region of chaos as the parameter a increases. A complicated variety of limit cycles is on the right side of the band. When a decreases from a relatively large value, the symmetry

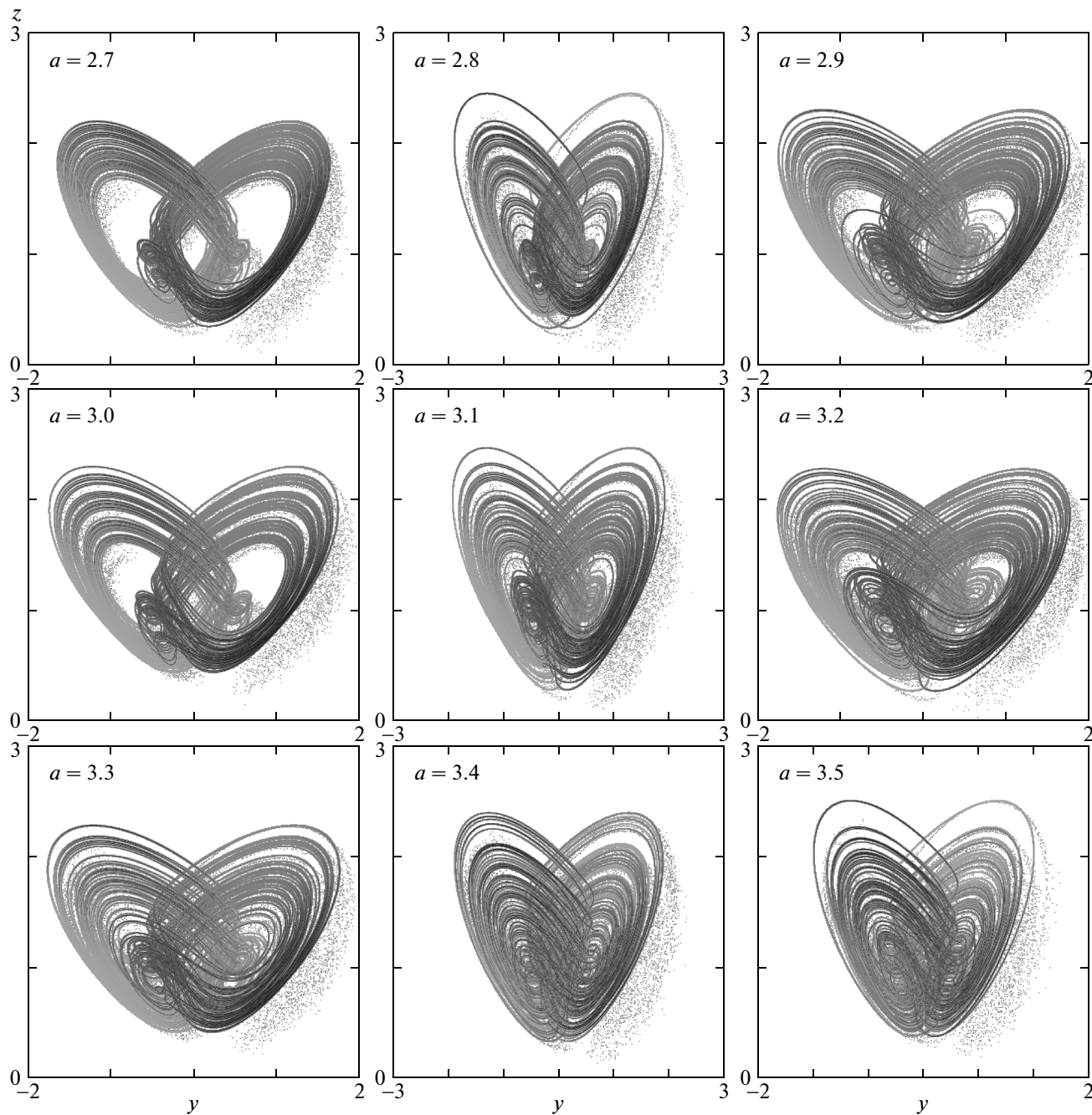


Fig. 5. Attractor merging and remerging at $b = 0.28$ and $c = 0.05$

of the attractor is broken, and a symmetric limit cycle turns into a symmetric pair of limit cycles, and then forms a symmetric pair of strange attractors as shown in Fig. 6. Eventually, the strange attractors merge to form a symmetric attractor that then becomes hyperchaotic.

This four-dimensional system shows a typical be-

havior for rotationally symmetric flows, where chaotic and hyperchaotic regions are surrounded by periodic regions, and hence the chaotic attractors usually arise from a symmetric pair of limit cycles, and then the attractors merge until the system eventually becomes hyperchaotic. No special bifurcation appears to accompany the transition of chaos to hyperchaos.

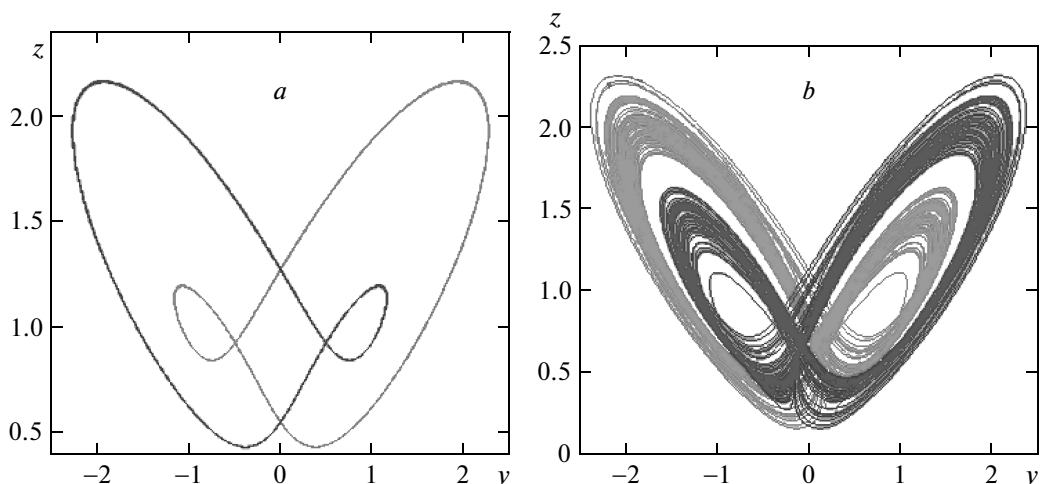


Fig. 6. Symmetric pair of coexisting limit cycles and strange attractors projected onto the yz plane for $b = 0.8$, $c = 0.05$ with the initial conditions $(\pm 1, \pm 1, 1, \pm 1)$ (a) $a = 4$ with LEs $(0, -0.0156, -0.1132, -2.3630)$, (b) $a = 2.5$ with LEs $(0.0208, 0, -0.0486, -2.1035)$

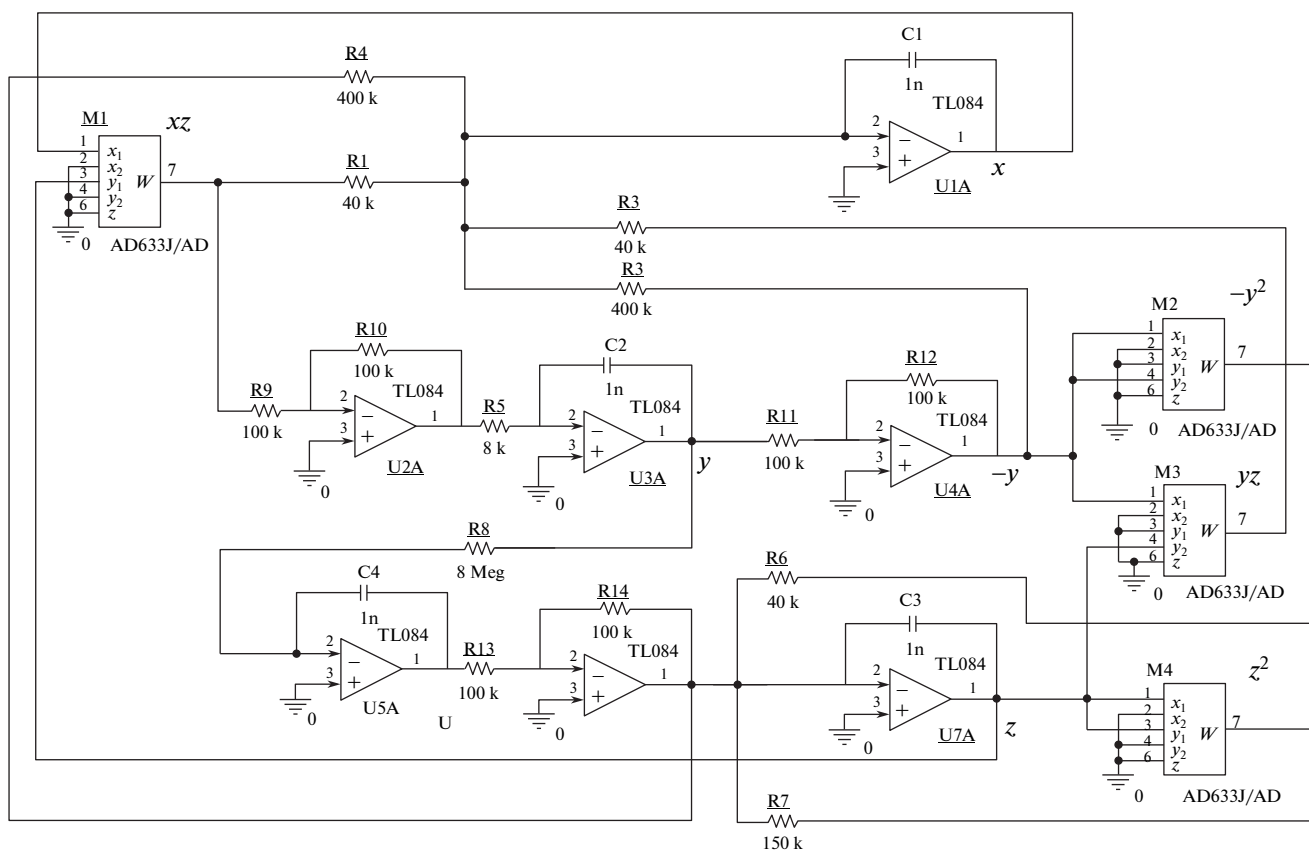


Fig. 7. Circuit realization of hyperchaotic system (2)

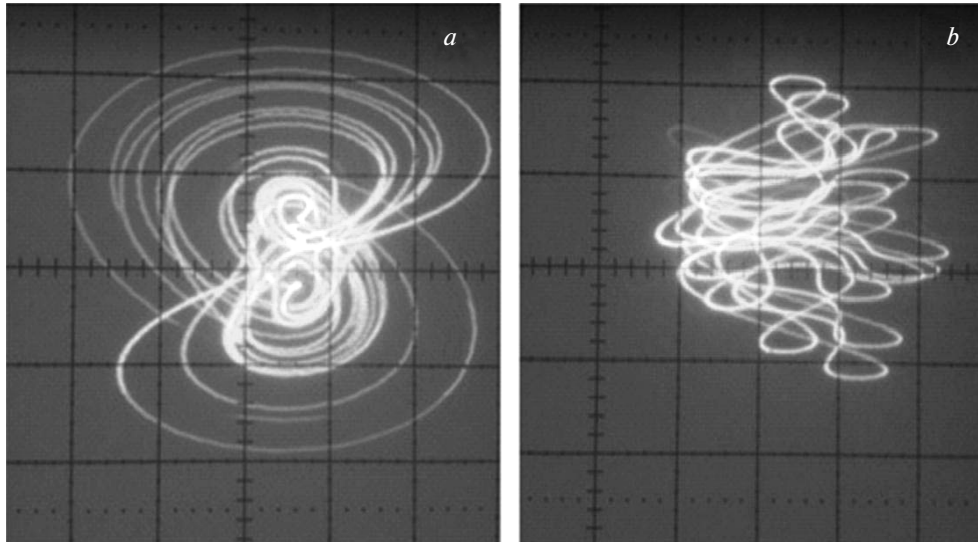


Fig. 8. Hyperchaotic attractor of system (2) with $a = 5$, $b = 0.28$, and $c = 0.05$ observed by oscilloscope: (a) xy plane, (b) zu plane, to compare with the prediction in Fig. 1

4. CIRCUIT IMPLEMENTATION

A circuit that models this hyperchaotic system was constructed to confirm the numerical predictions. The circuit equations are given by

$$\begin{aligned} \dot{x} &= \frac{1}{R_2 C_1} y - \frac{1}{10 R_1 C_1} x z - \\ &\quad - \frac{1}{10 R_3 C_1} y z + \frac{1}{R_4 C_1} u, \\ \dot{y} &= \frac{1}{10 R_5 C_2} x z, \\ \dot{z} &= \frac{1}{10 R_6 C_3} y^2 - \frac{1}{10 R_7 C_3} z^2, \\ \dot{u} &= -\frac{1}{R_8 C_4} y. \end{aligned} \tag{5}$$

Resistors R_5 , R_7 , and R_8 are made variable to change the parameters a , b , and c such that the dynamic regions in Fig. 3 could be tested. The circuit schematic is given in Fig. 7, and the resulting oscilloscope traces are shown in Fig. 8.

The system gives the maximum hyperchaos at $a = 5$, $b = 0.28$, and $c = 0.05$, which corresponds to the circuit values $C_1 = C_2 = C_3 = C_4 = 1$ nF,

$$R_1 = R_3 = R_6 = 40 \text{ k}\Omega, \quad R_2 = R_4 = 400 \text{ k}\Omega,$$

$$R_5 = 8 \text{ k}\Omega, \quad R_7 = 150 \text{ k}\Omega, \quad R_8 = 8 \text{ M}\Omega,$$

$$R_9 = R_{10} = R_{11} = R_{12} = R_{13} = R_{14} = 100 \text{ k}\Omega.$$

The multipliers are AD633JN, and the operational amplifiers are TL084. The circuit is powered by ± 9 volts.

The predictions in Fig. 3 were confirmed in this practical implementation when a varies between 1 to 10, and b between 0 to 1, with $c = 0.05$. In circuit values, this corresponds to R_5 varying from 40 k Ω to 4 k Ω and R_7 from 400 k Ω to 40 k Ω , with $R_8 = 8$ M Ω . As R_7 increases, the parameter b decreases, and the system goes through a limit cycle, torus, and chaos before reaching hyperchaos as predicted. As a varies from 2.2 to 2.89 ($R_5 = 18181 \Omega$ to 13840 Ω), coexisting strange attractors occur as expected. In the practical implementation, these varying values were implemented by replacing the correspondent resistor with a potentiometer.

5. CONCLUSION

A four-dimensional system with an infinite line of equilibrium points is found to have hyperchaotic solutions and a relatively large region of bistability in the parameter space where a symmetric pair of strange attractors coexists, then eventually merge and evolve into a symmetric hyperchaotic attractor at some particular parameter combinations. The results of a physical circuit agree with the numerical analysis.

This work was supported by the Jiangsu Overseas Research & Training Program for University Prominent Young and Middle-aged Teachers and Presidents, the 4th 333 High-level Personnel Training Project (Su Talent [2011] № 15) of Jiangsu Province, the National Science Foundation for Postdoctoral General

Program and Special Founding Program of People's Republic of China (Grant № 2011M500838 and Grant № 2012T50456) and Postdoctoral Research Foundation of Jiangsu Province (Grant № 1002004C).

REFERENCES

1. E. N. Lorenz, *J. Atmos. Sci.* **20**, 130 (1963).
2. G. Van der Schrier and L. R. M. Maas, *Phys. Nonlinear Phenom.* **141**, 19 (2000).
3. J. C. Sprott, *Phys. Rev. E* **50**, R647 (1994).
4. B. Ruy, *Int. J. Bifurcat. Chaos* **17**, 4285 (2007).
5. G. Qi and G. Chen, *Phys. Lett. A* **352**, 386 (2006).
6. S. Jafari and J. C. Sprott, *Chaos, Solitons & Fractals* **57**, 79 (2013).
7. C. Li and J. C. Sprott, *Phys. Lett. A* **378**, 178 (2014).
8. T. V. Gevorgyan, A. R. Shahinyan, L. Y. Chew, and F. Y. Kryuchkyan, *Phys. Rev. E* **88**, 022910 (2013).
9. R. K. Yadav, M. K. Verma, and P. Wahi, *Phys. Rev. E* **85**, 036301 (2012).
10. O. E. Rössler, *Phys. Lett. A* **71**, 155 (1979).
11. Z. Wang, S. Cang, E. O. Ochola, and Y. Sun, *Nonlinear Dyn.* **69**, 531 (2012).
12. C. Li and J. C. Sprott, *Int. J. Bifurcat. Chaos* **24**, 1450034 (2014).
13. G. Si, H. Cao, and Y. Zhang, *Chin. Phys. B* **20**, 010509 (2011).
14. G. Qi, A. Michaël van Wyk, B. J. van Wyk, and G. Chen, *Phys. Lett. A* **372**, 124 (2008).
15. Q. Li, S. Hu, and S. Tang, *Int. J. Circ. Theor. Appl.* DOI: 10.1002/cta.1912 (2013).